A stable dual pairing summation-by-parts method for sediment transport model with well-posed boundary conditions

Rudi Prihandoko[1] Stephen Roberts[2] Kenneth Duru[3]
Christopher Zoppou[4] Kenny Wiratama[5]

(Received 21 February 2025; revised 26 November 2025)

Abstract

We develop a dual pairing summation-by-parts operator with Godunov flux splitting for the sediment transport model. The required number, location, and form of boundary conditions are determined via the energy method at the continuous level. Stability of the initial boundary value problem is rigorously established. At the discrete level the boundary conditions are weakly enforced via penalty terms. Stability of the numerical model is demonstrated through a discrete energy estimate that mimics the continuous energy. Numerical experiments are conducted to verify the analysis.

DOI:10.21914/anziamproc.v66.19622 Published 2026-02-03, as part of the Proceedings of the 22nd Biennial Computational Techniques and Applications Conference. ISSN 1445-8810. (Print two pages per sheet of paper.)

Contents

1 Introduction

Understanding sediment transport in shallow water environments is critical for a wide range of environmental and engineering applications, including coastal management, riverbed formation, and erosion prediction. The shallow water wave equation describes the flow of water in environments where the water depth is much smaller than the wavelength, and serves as a fundamental model for simulating these dynamics. However, translating this understanding into accurate sediment transport models remains a complex challenge due to the interplay between hydrodynamic forces and morphodynamics solid transport discharge. Many authors have developed numerical models to simulate sediment transport in shallow water environments. These models typically involve solving the shallow water wave equation coupled with a sediment transport equation [19, 15, 16, 17, 7, 2].

There are many different equations to model the sediment transport: Grass equation [4]; Meyer-Peter and Müller equation [11]; van Rijn's equation [15, 16, 17]; Nielsen's equation [12]; Kalinske's equation [6]. Most of the models

are controlled by critical shear stress, which determines whether the sediment will be transported or not. The Meyer-Peter and Müller equation, van Rijn's equation, Nielsen's equation, and Kalinske's equation are examples of such models. In these models, the critical shear stress is determined experimentally and depends on the sediment properties such as size, density, and shape. In contrast, the Grass equation [4] is not based on the critical shear stress, but directly relates the sediment transport rate to the flow velocity. For this reason, we choose the Grass equation to model the sediment transport in this study; it is also simpler and computationally cheaper than the other models.

A key challenge in accurately approximating bedload sediment transport is that the interaction between fluid flow and sediment transport is often weak, leading to a wide range of time scales in the system. This makes the numerical simulation of sediment transport in shallow water environments particularly challenging. The low order numerical schemes are very diffusive while the high order schemes are often unstable [2].

In this article, we use a high-order numerical method based on dual pairing summation-by-parts (SBP) operators [18, 10] to discretize the model. In the following sections, we present the continuous stability analysis, well-posedness of the boundary conditions, and the discrete stability analysis. The stability of the numerical model is analyzed using the energy method, and the well-posedness of the boundary conditions is established. We do the analysis in a one-dimensional linearised systems. To ensure stability, we apply penalty terms to weakly enforce the boundary conditions. This technique provides a framework for achieving high accuracy while preserving the stability of the model, guaranteed by the energy method [1, 8, 9, 13].

The rest of the article is as follows. In Section 2, we prove the continuous stability of the linearised model including the number and location of the boundary conditions. In Section 3, we present the discrete stability analysis as well as the penalty terms. In Section 4, we present numerical experiments to verify the stability and accuracy of the model.

2 Continuous stability

One-dimensional linearised model and Riemann invariant Consider the one-dimensional shallow water wave equation coupled with the sediment transport equation:

$$\partial_t h + \partial_x(uh) = 0\,, \tag{1a}$$

$$\partial_t(uh) + \partial_x(u^2h + \frac{1}{2}gh^2) = -gh\partial_x z\,, \tag{1b}$$

$$\partial_t z + \partial_x(q_b) = 0\,, \tag{1c}$$

where x is the spatial variable, $t \geq 0$ is time, $h(x,t) > 0$ and $u(x,t)$ are water depth and depth averaged fluid velocity, respectively, $z(x,t)$ is sediment depth, and g is the gravitational acceleration. The Grass equation for the sediment is

$$q_b = \frac{A}{1-\varphi}|u|^n u\,, \tag{2}$$

where φ is the porosity of the sediment, A is interaction between the sediment and the fluid, and $0 \leq n \leq 3$ is an integer. The value of parameter A is determined experimentally; A closer to zero implies weak interaction between the sediment and the fluid, and A closer to one means strong interaction between the sediment and the fluid. Usually $n = 2$, as suggested by Castro Diaz et al. [2], and $A = 0.0005$, as suggested by Wren et al. [19].

Because of the nonlinear evolution equation (1c) for the sediment depth z, and the source term in the right hand side of the momentum equation (1b), the coupled equation (1a)–(1c) are much more complicated than the nonlinear shallow water equation. However, for a stationary sediment depth profile with $\partial_t z \equiv 0$ we recover the standard 1D nonlinear shallow water equation.

We linearise our model by substituting $h = H + \tilde{h}$, $u = U + \tilde{u}$, $z = Z + \tilde{z}$, where $\tilde{h}, \tilde{u}$ and $\tilde{z}$ denote small perturbations of the constant water depth $H > 0$, fluid velocity U and sediment depth Z, respectively.

Substituting (2) into (1c) and linearising the equation, we have

$$\partial_t \tilde{h} + U\partial_x \tilde{h} + H\partial_x \tilde{u} = 0\,, \tag{3a}$$

$$\partial_t \tilde{u} + g\partial_x \tilde{h} + U\partial_x \tilde{u} = -g\partial_x \tilde{z}\,, \tag{3b}$$

$$\partial_t \tilde{z} + \frac{A}{1-\varphi} 3U^2 \partial_x \tilde{u} = 0\,. \tag{3c}$$

In (3c), if $U = 0$ we have $\partial_t \tilde{z} = 0$ and hence our system can be reduce to a linearised shallow water wave equation with source terms. Throughout this manuscript, we assume non-zero U.

Rewriting equation (3) in matrix form, we have

$$\partial_t \mathbf{p} = D\mathbf{p}\,, \quad D = -M\partial_x\,, \quad M = \begin{bmatrix} U & H & 0 \\ g & U & g \\ 0 & k & 0 \end{bmatrix}, \quad k = \frac{A}{1-\varphi} 3U^2, \tag{4}$$

where $\mathbf{p} = \begin{bmatrix} \tilde{h} & \tilde{u} & \tilde{z} \end{bmatrix}^\top$.

We now introduce the dimensionless variables $\mathbf{q} = \begin{bmatrix} h^* & u^* & z^* \end{bmatrix}^\top = W^{-1}\mathbf{p}$ to ensure dimensional consistencies in our calculation. Here W is a diagonal matrix $W = \mathrm{diag}(\sqrt{H}, \sqrt{g}, \sqrt{k})$. Furthermore, we drop the star for simplicity. Then, we have the symmetrized matrix form

$$\partial_t \mathbf{q} = D\mathbf{q}\,, \quad D = -\widetilde{M}\partial_x\,, \quad \widetilde{M} = W^{-1}MW = \begin{bmatrix} U & \sqrt{gH} & 0 \\ \sqrt{gH} & U & \sqrt{gk} \\ 0 & \sqrt{gk} & 0 \end{bmatrix}. \tag{5}$$

Since M and $\widetilde{M}$ are similar, they have the same eigenvalues, while the eigenvectors are related to each other by a factor of W. Note that $\widetilde{M}$ is symmetric; hence it has real eigenvalues. We can easily check that all the eigenvalues are distinct via the discriminant of the characteristic polynomial of the matrix. Distict eigenvalues mean that the system is strictly hyperbolic and implies the diagonalizability of matrix $\widetilde{M}$ as well as the original matrix M.

Interesting boundary conditions for this type of problem are transmissive boundary conditions. These boundary conditions are closely related to the Riemann invariants of the system, which involve the eigenvectors of the matrix. In the next section, we see that for non-zero depth averaged velocity, the number of boundary conditions is influenced by the sign of the depth averaged velocity, but not the size of the flow (this is different from the shallow water wave equation, which depends on whether the flow is super or sub-critical).

Given that the matrix is diagonalizable, we could find the roots of the characteristic polynomial of the matrix M to determine the sign of the eigenvalues from which the number and type of boundary conditions follow. While algebraically factoring the characteristic polynomial is challenging, the computation can be done numerically.

Well-posedness We consider (5) in a bounded domain with initial and boundary conditions. Let $\Omega = [0, L]$ be our domain of interest and $\Gamma = \{0, L\}$ be the boundary points. Consider the initial boundary value problem (IBVP)

$$\partial_t \mathbf{q} = D\mathbf{q}\,, \quad x \in \Omega\,, \quad t \geq 0\,, \tag{6a}$$
$$\mathbf{q}(x, 0) = \mathbf{f}(x)\,, \quad x \in \Omega\,, \tag{6b}$$
$$\mathcal{B}\mathbf{q} = \mathbf{b}(t)\,, \quad x \in \Gamma\,, \quad t \geq 0\,, \tag{6c}$$

where $\mathcal{B}$ is a linear boundary operator, $\mathbf{b}$ is the boundary data and $\mathbf{f} \in L^2(\Omega)$ is the initial condition. We aim for IBVP (6) to be well-posed within our choice of $\mathcal{B}$.

Define an inner product and the induced norm:

$$(\mathbf{p}, \mathbf{q}) = \int_\Omega \mathbf{q}^\top \mathbf{p}\, dx\,, \quad \|\mathbf{q}\|^2 = (\mathbf{q}, \mathbf{q})\,. \tag{7}$$

We then introduce a function space which relates to the boundedness of the differential operator D:

$$\mathbb{V} = \{\mathbf{q} \mid \mathbf{q}(x) \in \mathbb{R}^3\,; \|\mathbf{q}\| < \infty\,, 0 \leq x \leq L\,; \mathcal{B}\mathbf{q}(x) = 0\,, x \in \Gamma\}\,.$$

We also need to define the well-posedness of our IBVP and the semi-boundedness of the operator.

Definition 1. The IBVP (6) is well-posed if for homogeneous boundary data $\mathbf{b}(t) = 0$ there exists a unique solution $\mathbf{q}$ satisfying

$$\|\mathbf{q}(\cdot, t)\| \leq \kappa e^{\nu t} \|\mathbf{f}\|, \quad \|\mathbf{f}\| < \infty,$$

for some constants $\kappa > 0$ and $\nu \in \mathbb{R}$ independent of $\mathbf{f}$.

Definition 2. The operator D is semi-bounded in the function space $\mathbb{V}$ if it satisfies

$$(\mathbf{q}, D\mathbf{q}) \leq \mu \|\mathbf{q}\|^2, \quad \mu \in \mathbf{R}.$$

The operator D is maximally semi-bounded if it is semi-bounded in the function space $\mathbb{V}$ but not semi-bounded in any space with fewer boundary conditions.

The maximally semi-boundedness of differential operator D is a necessary and sufficient condition for the well-posedness of the IBVP (6), as shown by Gustafsson et al. [5]. We ensure the well-posedness of the IBVP (6) by proving that the differential operator D is maximally semi-bounded. The following lemma is similar to our previous work [14], except there is an additional sediment equation, and hence the matrix M is larger.

Lemma 3. *Consider the differential operator* D *with the constant coefficients and matrix* $\widetilde{M}$ *given in* (5)*, the inner product defined in* (7) *and* $\mathbf{q}^\top \mathbf{q} > 0$ *for all nonzero* $\mathbf{q} \in \mathbb{R}^3$*. If the matrix* $\widetilde{M}$ *is symmetric,* $\widetilde{M} = \widetilde{M}^\top$*, and* $\left(\mathbf{q}^\top \widetilde{M} \mathbf{q}\right)\Big|_0^L \geq 0$*, then* D *is semi-bounded.*

The next course of action is to derive boundary operator $\mathcal{B}$ such that $\{\mathcal{B}\mathbf{q}(x) = 0, x \in \Gamma\}$ with the minimal number of boundary conditions such that the boundary term is never negative or equivalently, $(\mathbf{q}^\top \widetilde{M} \mathbf{q})\Big|_0^L \geq 0$.

Let the energy related to this linearised PDE be

$$\mathsf{E} := \int_\Omega (h^2 + u^2 + z^2)\, \mathrm{d}x = \|\mathbf{q}\|^2. \tag{8}$$

Recall the IBVP (6a), multiply it by $\mathbf{q}^\top$ and add its transpose, then integrate over the domain to obtain the energy estimate

$$\int_\Omega \left[\partial_t(\mathbf{q}^\top\mathbf{q}) + \partial_p(\mathbf{q}^\top\widetilde{M}\mathbf{q})\right] \mathrm{d}x = 0\,, \tag{9}$$

via integration by parts. Furthermore, by the divergence theorem

$$\frac{\mathrm{d}}{\mathrm{d}t}\|\mathbf{q}\|^2 + \mathbf{q}^\top\widetilde{M}\mathbf{q}\Big|_{x=0}^{x=L} = 0\,. \tag{10}$$

We want to have the energy bounded. So, it is sufficient to have $\frac{\mathrm{d}}{\mathrm{d}t}\|\mathbf{q}\|^2$ be negative. This is achieved by having appropriate boundary conditions.

The number of boundary conditions Finding the eigenvalues of the matrix is non-trivial, even with numerical methods for approximating tridiagonal matrix eigenvalues. However, we determine their signs by analysing the characteristic polynomial. The polynomial characteristic of matrix $\widetilde{M}$ is $\lambda^3 - 2U\lambda^2 + (-Hg + U^2 - gk)\lambda + Ugk$ with discriminant

$$\begin{aligned}
&4H^3g^3 - 8H^2U^2g^2 + 4HU^4g + 12H^2g^3k \\
&\quad + 20HU^2g^2k + 12Hg^3k^2 + U^2g^2k^2 + 4g^3k^3 \\
&= 4\left[\left(\sqrt{gH}\right)^3 - U^2\sqrt{gH}\right]^2 + 12H^2g^3k + 20HU^2g^2k \\
&\quad + 12Hg^3k^2 + U^2g^2k^2 + 4g^3k^3.
\end{aligned}$$

The discriminant of this polynomial can be shown to be positive for $k > 0$ and hence three different real roots are guaranteed. Let $\lambda_1 > \lambda_2 > \lambda_3$ be the roots of the characteristic polynomial. Then

$$\lambda_1 + \lambda_2 + \lambda_3 = 2U\,, \tag{11a}$$

$$\lambda_1\lambda_2 + \lambda_1\lambda_3 + \lambda_2\lambda_3 = -Hg + U^2 - gk, \tag{11b}$$
$$\lambda_1\lambda_2\lambda_3 = -Ugk. \tag{11c}$$

If $U > 0$, from (11c), we have an odd number of negative eigenvalues since $g, k > 0$. From (11a) it is not possible to have three negative eigenvalues, so there must be one negative eigenvalue. So we will have one negative eigenvalue and two positive eigenvalues. A similar argument is made for $U < 0$ but in this case there are two negative eigenvalues and one positive.

Recall that the number of boundary conditions on each boundary is determined by the sign of eigenvalues of $\widetilde{M}$. Negative eigenvalues of $\widetilde{M}$ will give us the number of boundary conditions on the left boundary, and positive eigenvalues of $\widetilde{M}$ will give us the number of boundary conditions on the right boundary. For $U > 0$, we have one negative eigenvalue and two positive eigenvalues. So, it is one boundary condition on the left and two boundary conditions on the right (inflow at $x = 0$). For $U < 0$, we have a similar case but with swapped boundary conditions (inflow at $x = L$). For either case, we need two boundary conditions on the inflow and one boundary condition on the outflow.

Let $\widetilde{M} = S\Lambda S^\top$ and $\Lambda = \operatorname{diag}(\lambda_1, \lambda_2, \lambda_3)$. Then, using a linear transformation $S^\top \mathbf{q} = \boldsymbol{w} = [w_1,\ w_2,\ w_3]^\top$, we rearrange the boundary terms (BT) in the diagonalized form:

$$\mathrm{BT} = \left(\lambda_1 w_1^2 + \lambda_2 w_2^2 + \lambda_3 w_3^2\right)\Big|_{x=0} - \left(\lambda_1 w_1^2 + \lambda_2 w_2^2 + \lambda_3 w_3^2\right)\Big|_{x=L}. \tag{12}$$

Case $U > 0$: left inflow, right outflow We have $\lambda_1 > \lambda_2 > 0$ and $\lambda_3 < 0$. We formulate the boundary conditions by

$$\{\mathcal{B}\mathbf{q}(x) = \mathbf{b}, x \in \Gamma\} \equiv \{w_1 - \beta_1 w_3 = b_1(t), w_2 - \beta_2 w_3 = b_2(t) \text{ at } x = 0; \\ w_3 - \alpha_1 w_1 - \alpha_2 w_2 = b_3(t) \text{ at } x = L\}, \tag{13}$$

where $\mathbf{b} = [b_1\ b_2\ b_3]^\top$ and $\beta_1, \beta_2, \alpha_1, \alpha_2 \in \mathbb{R}$ are boundary reflection coefficients. The parameters α_1, α_2, β_1, β_2 are constrained by the stability condition, as in the following lemma for which the proof is in Appendix A.

Lemma 4. *Consider the boundary term* BT *defined in* (12) *and the boundary conditions* (13) *with* $b = 0$ *for case* $U > 0$ *with* $\lambda_1 > \lambda_2 > 0 > \lambda_3$. *If both conditions* $\left(\frac{\lambda_1}{-\lambda_3}\right)\beta_1^2 + \left(\frac{\lambda_2}{\lambda_3}\right)\beta_2^2 \leq 1$ *and* $\left(\frac{-\lambda_3}{\lambda_1}\right)\alpha_1^2 + \left(\frac{-\lambda_3}{\lambda_2}\right)\alpha_2^2 \leq 1$ *are fulfilled, then the boundary term* BT *is negative.*

Case $U < 0$: right inflow, left outflow This case is similar to the $U > 0$ case, but flip the boundary conditions. All the conditions and the proof are similar.

3 Numerical scheme

In this section, we discretize the boundary conditions using dual pairing summation-by-parts (DP-SBP) operators and enforce stability with simultaneous approximation terms (SAT) as penalties.

Define a uniform grid $\{x_i\}_{i=0}^N$ with $x_0 = 0$ and $x_N = L$. Let $\Delta x = x_{i+1} - x_i$ be the grid spacing. Write $h_i = h(x_i, t)$, $u_i = u(x_i, t)$, $z_i = z(x_i, t)$, and $\mathbf{h} = [h_i]_{i=0}^N$, $\mathbf{u} = [u_i]_{i=0}^N$, $\mathbf{z} = [z_i]_{i=0}^N$. Write $\mathbf{p} = \begin{bmatrix}\mathbf{h} & \mathbf{u} & \mathbf{z}\end{bmatrix}^\top$.

Dual pairing SBP operator. An operator pair (D, P) is said to be a summation-by-parts (SBP) operator with order p along with a weighted inner product $\langle \cdot, \cdot \rangle_P$ if it has: a) quadrature properties, that is $\langle 1, \mathbf{f} \rangle_P \approx \int_\Omega \mathbf{f}\, dx$ for any function $\mathbf{f}$; b) discrete derivative property, that is $D\mathbf{f}(x) = \mathbf{f}'(x)$ for all polynomial $\mathbf{f}$ with degree less than or equal to p; and c) summation-by-parts property, that is

$$\langle D\mathbf{f}, \mathbf{g} \rangle_P + \langle \mathbf{f}, D\mathbf{g} \rangle_P = \mathbf{f}(x_N)\mathbf{g}(x_N) - \mathbf{f}(x_0)\mathbf{g}(x_0).$$

Along with the SBP operator, we define the dual pairing operator as follows.

Definition 5. The dual pairing operator (D_+, D_-) is a dual pairing operator of the SBP operator (D, P) if it satisfies the following properties for some function $\mathbf{f}$ and primitive $\mathbf{g}$.

1. Dual pairing property. That is $D = \frac{1}{2}(D_+ + D_-)$ and

$$\langle D_+ \mathbf{f}, \mathbf{g}\rangle_P + \langle \mathbf{f}, D_- \mathbf{g}\rangle_P = \mathbf{f}(x_N)\mathbf{g}(x_N) - \mathbf{f}(x_0)\mathbf{g}(x_0)\,.$$

2. Upwind property. That is, $\langle \mathbf{f}, (D_+ - D_-)\mathbf{f}\rangle_P \leq 0$ for all $\mathbf{f} \in \mathbb{R}^N$.

Discretization and penalty terms Let $f_\pm = f(\mathbf{p}_i) \pm \gamma \mathbf{p}_i$ be Godunov flux splitting [3] with $f = \mathbf{f}_+ + \mathbf{f}_-$ and where γ is the maximum absolute eigenvalue of the operator f. Let M be the matrix defined in (4). Let S be the orthogonal matrix that diagonalizes $\widetilde{M}$ from (5).

We use the dual pairing SBP operator to approximate the spatial derivative. We choose D_+ and D_- to be forward finite difference and backward finite difference operators, respectively. Let $D = (D_+\mathbf{f}_- + D_-\mathbf{f}_+)$. Let P be the diagonal matrix such that (D, P) is an SBP operator [10]. Hence the pair (D_+, D_-) is a dual pairing operator with respect to the SBP operator (D, P).

Incorporating penalty terms modifies the system:

$$\frac{d}{dt}\mathbf{p} + (M \otimes D)\mathbf{p} + \frac{\gamma}{2}[I \otimes (D_+ - D_-)]\mathbf{p} = \text{SAT}\,. \tag{14}$$

For the case $U > 0$,

$$\text{SAT} = -\frac{1}{2}(WS \otimes P^{-1}) \begin{bmatrix} \tau_1 \boldsymbol{e}_0(w_1 - \beta_1 w_3) \\ \tau_2 \boldsymbol{e}_0(w_2 - \beta_2 w_3) \\ \tau_3 \boldsymbol{e}_N(w_3 - \alpha_1 w_1 - \alpha_2 w_2) \end{bmatrix}. \tag{15}$$

For the case $U < 0$,

$$\text{SAT} = -\frac{1}{2}(WS \otimes P^{-1}) \begin{bmatrix} \tau_1 \boldsymbol{e}_0(w_1 - \alpha_1 w_2 - \alpha_2 w_3) \\ \tau_2 \boldsymbol{e}_N(w_2 - \beta_2 w_1) \\ \tau_3 \boldsymbol{e}_N(w_3 - \beta_3 w_2) \end{bmatrix}. \tag{16}$$

Matrix W is the rescaling matrix from (5), S is the matrix that diagonalises $\widetilde{M}$, and P is the diagonal matrix related to the DP SBP operator.

Introduce the discrete weighted L_2-norm:

$$\|q\|^2 = q^\top (I \otimes P) q \geq 0, \tag{17}$$

with the associated discrete energy $E = \|q\|$. We now show that the energy is non-increasing to ensure the stability of the system.

Theorem 6. *Consider the semi-discrete approximation of the system (14) with the penalty terms and $U > 0$. If the penalty terms τ_1, τ_2 and τ_3 are chosen such that the following conditions are satisfied:*

$$2(\tau_1 + \lambda_1) < -\lambda_3 \quad \textit{and} \quad 2\lambda_1\lambda_3 + 2\lambda_3\tau_1 - \beta_1^2\tau_1^2 > 0, \tag{18a}$$

$$2(\tau_2 + \lambda_2) < -\lambda_3, \quad \textit{and} \quad 2\lambda_2\lambda_3 + 2\lambda_3\tau_2 - \beta_2^2\tau_2^2 > 0, \tag{18b}$$

$$8\lambda_1\lambda_2\lambda_3 + 8\lambda_1\lambda_2\tau_3 - 2(\lambda_1\alpha_2^2 + \lambda_2\alpha_1^2)\tau_3^2 > 0, \tag{18c}$$

then the energy of the system is non-increasing, or equivalently,

$$\frac{d}{dt}\|q\|^2 \leq 0. \tag{19}$$

The proof of this Lemma is in Appendix B.

4 Numerical experiments

In this section we present numerical experiments to demonstrate the stability of the proposed scheme. We use $[0, L]$ as the domain of interest with $L = 10\,\mathrm{m}$, $H = 1\,\mathrm{m}$, and $g = 9.81\,\mathrm{m/s^2}$. We use $U = 1$ so that $x = 0$ is the inflow boundary and $x = L$ is the outflow boundary. We also use the following parameters for the numerical experiments: $A = 0.0005$, $\varphi = 0.3$, $t = 0$. The initial condition is a Gaussian profile $f(x) = \frac{1}{2}\exp\left[-\frac{1}{2}\frac{(x-L/2)^2}{3^2}\right]$.

Let $M = T\Lambda T^{-1}$ be diagonalization of M. The transmissive boundary for $U > 0$ is

$$\omega_1 = 0, \omega_2 = 0 \text{ at } x = 0, \text{ and } \omega_3 = 0 \text{ at } x = L,$$

where $\omega_1, \omega_2, \omega_3$ are the eigenvectors of the matrix T.

The discrete model (14) is integrated in time using the classical fourth-order Rung–Kutta method with a time step of

$$\Delta t = Cr \frac{\Delta x}{\max_i |\lambda_i|},$$

where $Cr = 0.25$ is the Courant–Friedrichs–Lewy number. We use DP-SBP with the order of accuracy of 4.

We compute the energy throughout the simulation for $N = 1601$, to verify the stability of the scheme. The results are shown in Figure 1a. The energy is non-increasing, which confirms the stability of the proposed scheme. The energy lost in around $t = 10$ and $t = 20$ is due to the waves moving out of the domain. The final energy loss is not presented here. Figure 1b shows that there is energy loss in small amount before the waves move out of the domain.

Convergence test We performed a convergence test against the exact solution to verify the order of accuracy of the proposed scheme. We used the exact solution given by decomposing the matrix M into the eigenvectors of the matrix T:

$$\frac{dw_i}{dt} + \gamma_i \frac{dw_i}{dx} = 0, \tag{20}$$

where γ_i is the eigenvalue of the matrix T. The exact solution is

$$w_i(x, t) = w_i(x - \gamma_i t, 0), \tag{21}$$

where $\boldsymbol{w}(x, 0) = S^{-1}\boldsymbol{q}(x, 0)$ is the initial condition.

We computed the error in the L^2 norm for different grid sizes. The results are shown in Figure 2 and Table 1.

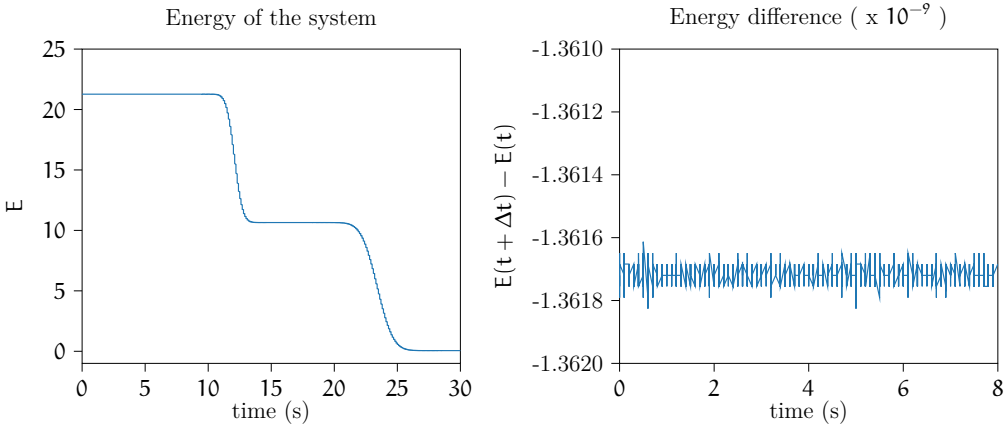

(a) (b)

Figure 1: (a) The energy throughout the simulation for $N = 1601$. The energy is non-increasing, which confirms the stability of the proposed scheme. (b) Energy difference in the first 8 seconds.

Table 1: Convergence test for the proposed scheme. The error in the L^2 norm is shown for different grid sizes. The order of accuracy is approximately 4.

N	h error	rate	u error	rate	z error	rate
51	1.05e-01	—	3.28e-01	—	3.23e-04	—
101	1.38e-02	2.92	4.33e-02	2.92	4.29e-05	2.91
201	9.36e-04	3.88	2.93e-03	3.88	2.28e-06	4.24
401	5.84e-05	4.00	1.83e-04	4.00	1.24e-07	4.20
801	3.63e-06	4.01	1.14e-05	4.01	7.41e-09	4.06
1601	2.27e-07	4.00	7.11e-07	4.00	4.61e-10	4.01
3201	1.42e-08	4.00	4.44e-08	4.00	2.89e-11	4.00
6401	8.85e-10	4.00	2.78e-09	4.00	1.81e-12	4.00

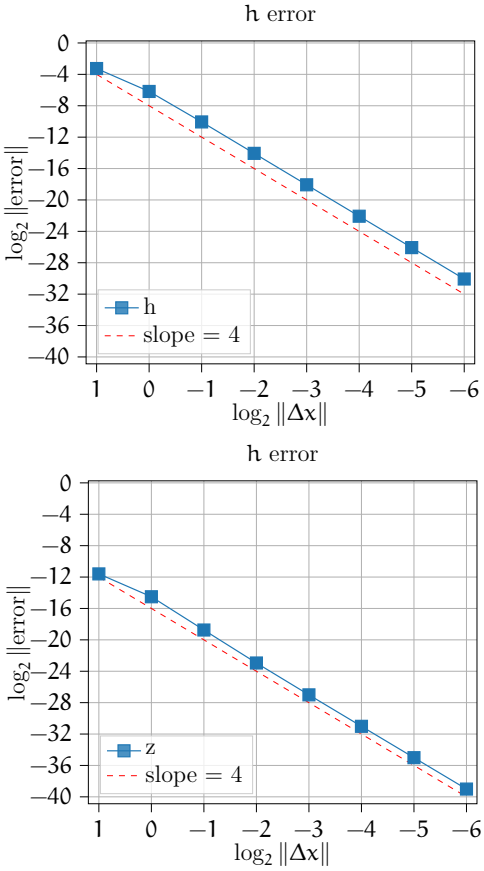

Figure 2: Convergence test for the proposed scheme. The error in the L^2 norm is plotted against the grid size. The slope of the error is approximately 4, which confirms the fourth-order accuracy of the proposed scheme.

5 Conclusion

In this article, we have proposed a stable numerical scheme with well-posed boundary conditions. The analysis of the proposed scheme has shown that the energy is non-increasing for suitable boundary conditions. The number of boundary conditions is influenced by the sign of the depth averaged velocity of the flow, but not the size. The shallow water wave equation can be retrieved as a special case of the proposed scheme. The numerical experiments have confirmed the stability and the order of accuracy of the proposed scheme.

Acknowledgements This research is conducted as part of doctoral study funded by Indonesian Endowment Fund for Education (LPDP) of Indonesia. The last author acknowledges support from the National Research Foundation of Korea, South Korea (NRF-2023R1A2C1006845).

References

[1] M. H. Carpenter, D. Gottlieb, and S. Abarbanel. "Time-stable boundary conditions for finite-difference schemes solving hyperbolic systems: methodology and application to high-order compact schemes". In: *J. Comput. Phys.* 111.2 (1994), pp. 220–236. DOI: 10.1006/jcph.1994.1057 (cit. on p. C148).

[2] M. J. Castro Díaz, E. D. Fernández-Nieto, and A. M. Ferreiro. "Sediment transport models in shallow water equations and numerical approach by high order finite volume methods". In: *Comput. Fluids* 37.3 (2008), pp. 299–316. DOI: 10.1016/j.compfluid.2007.07.017. (Cit. on pp. C147, C148, C149).

[3] S. K. Godunov. "A finite difference method for the numerical computation of discontinuous solutions of the equations of fluid dynamics". In: *Mat. Sbornik* 47.89 (1959). (English translation: I. Bohachevsky, *Soviet Math. Dok.*, 11 (1969), pp. 494–497 https://hal.science/hal-01620642v1/), pp. 271–306. URL: https://www.mathnet.ru/eng/sm4873 (cit. on p. C156).

[4] A. J. Grass. *Sediment Transport by Waves and Currents*. Science and Engineering Research Council (Great Britain), London Centre for Marine Technology. University College, London, Dept. of Civil Engineering. Report No. FL29. 1981 (cit. on pp. C147, C148).

[5] B. Gustafsson, H.-O. Kreiss, and J. Oliger. *Time dependent problems and difference methods*. John Wiley & Sons, 2013. DOI: 10.1002/9781118548448 (cit. on p. C152).

[6] A. A. Kalinske. "Criteria for determining sand-transport by surface-creep and saltation". In: *Eos, Trans. Am. Geophys. Union* 23 (2042), pp. 639–643. DOI: 10.1029/TR023i002p00639 (cit. on p. C147).

[7] X. Liu and A. Beljadid. "A coupled numerical model for water flow, sediment transport and bed erosion". In: *Comput. Fluids* 154 (2017), pp. 273–284. DOI: 10.1016/j.compfluid.2017.06.013. (Cit. on p. C147).

[8] T. Lundquist and J. Nordström. "The SBP-SAT technique for time-discretization". In: *21st AIAA Computational Fluid Dynamics Conference*. DOI: 10.2514/6.2013-2834. (Cit. on p. C148).

[9] T. Lundquist and J. Nordström. "The SBP-SAT technique for initial value problems". In: *J. Comput. Phys.* 270 (2014), pp. 86–104. DOI: 10.1016/j.jcp.2014.03.048. (Cit. on p. C148).

[10] K. Mattsson. "Diagonal-norm upwind SBP operators". In: *J. Comput. Phys.* 335 (2017), pp. 283–310. DOI: 10.1016/j.jcp.2017.01.042. (Cit. on pp. C148, C156).

[11] E. Meyer-Peter and R. Müller. *Formulas for bed-load transport*. TU Delft Repository. 1948. URL: https://resolver.tudelft.nl/uuid:4fda9b61-be28-4703-ab06-43cdc2a21bd7/ (cit. on p. C147).

[12] P. Nielsen. *Coastal Bottom Boundary Layers and Sediment Transport*. Vol. 4. Advanced Series on Ocean Engineering. World Scientific, 1992. DOI: 10.1142/1269. (Cit. on p. C147).

[13] J. Nordström and M. H. Carpenter. "High-Order finite difference methods, multidimensional linear problems, and curvilinear coordinates". In: *J. Comput. Phys.* 173.1 (2001), pp. 149–174. DOI: 10.1006/jcph.2001.6864. (Cit. on p. C148).

[14] R. Prihandoko, K. Duru, S. Roberts, and C. Zoppou. "On well-posed boundary conditions and energy stable finite-volume method for the linear shallow water wave equation". In: *ANZIAM J.* 66.3 (2024), pp. 181–200. DOI: 10.1017/S1446181124000191 (cit. on p. C152).

[15] L. C. van Rijn. "Sediment transport, Part I: Bed load transport". In: *J. Hyd. Eng.* 110.10 (1984), pp. 1431–1456. DOI: 10.1061/(ASCE)0733-9429(1984)110:10(1431) (cit. on p. C147).

[16] L. C. van Rijn. "Sediment transport, Part II: Suspended load transport". In: *J, Hyd. Eng.* 110.11 (1984), pp. 1613–1641. DOI: 10.1061/(ASCE)0733-9429(1984)110:11(1613). (Cit. on p. C147).

[17] L. C. van Rijn. "Sediment transport, Part III: Bed forms and alluvial roughness". In: *J. Hyd. Eng.* 110.12 (1984), pp. 1733–1754. DOI: 10.1061/(ASCE)0733-9429(1984)110:12(1733). (Cit. on p. C147).

[18] C. Williams and K. Duru. "Full-spectrum dispersion relation preserving summation-by-parts operators". In: *SIAM J. Numer. Anal.* 62.4 (2024), pp. 1565–1588. DOI: 10.1137/23M1586471. (Cit. on p. C148).

[19] D. G. Wren, R. A. Kuhnle, E. J. Langendoen, and T. O. McAlpin. "Sediment transport and bed topography for realistic unsteady flow hydrographs of varying length in a laboratory flume". In: *J. Hyd. Eng.* 150.4, 04024018 (2024). DOI: 10.1061/JHEND8.HYENG-13769. (Cit. on pp. C147, C149).

A Proof of Lemma 4

At $x = 0$ let $w_1 = \beta_1 w_3$ and $w_2 = \beta_2 w_3$. We have

$$BT\Big|_{x=0} = \lambda_1 w_1^2 + \lambda_2 w_2^2 + \lambda_3 w_3^2 = (\lambda_1 \beta_1^2 + \lambda_2 \beta_2^2 + \lambda_3) w_3^2 .$$

Notice that $\lambda_1 \beta_1^2 + \lambda_3 + \lambda_2 \beta_2^2 \leq 0$ is equivalent to $\left(\frac{\lambda_1}{-\lambda_3}\right) \beta_1^2 + \left(\frac{\lambda_2}{\lambda_3}\right) \beta_2^2 \leq 1$ which leads to $BT|_{x=0} \leq 0$.

At $x = L$ let $w_3 = \alpha_1 w_1 + \alpha_2 w_2$. We have

$$BT\Big|_{x=L} = \begin{bmatrix} w_1 & w_2 \end{bmatrix} \begin{bmatrix} \lambda_1 + \lambda_3 \alpha_1^2 & \lambda_3 \alpha_1 \alpha_2 \\ \lambda_3 \alpha_1 \alpha_2 & \lambda_2 + \lambda_3 \alpha_2^2 \end{bmatrix} \begin{bmatrix} w_1 \\ w_2 \end{bmatrix} = \begin{bmatrix} w_1 & w_2 \end{bmatrix} B_L \begin{bmatrix} w_1 \\ w_2 \end{bmatrix} .$$

Since $\left(\frac{-\lambda_3}{\lambda_1}\right)\alpha_1^2 + \left(\frac{-\lambda_3}{\lambda_2}\right)\alpha_2^2 \le 1$, we have $\lambda_1\lambda_2 + \lambda_2\lambda_3\alpha_1^2 + \lambda_1\lambda_3\alpha_2^2 \ge 0$, which is equivalent to the determinant of the matrix B_L being non-negative. We also have

$$1 \ge \left(\frac{-\lambda_3}{\lambda_1}\right)\alpha_1^2 + \left(\frac{-\lambda_3}{\lambda_2}\right)\alpha_2^2 \ge \left(\frac{-\lambda_3}{\lambda_1+\lambda_2}\right)\alpha_1^2 + \left(\frac{-\lambda_3}{\lambda_1+\lambda_2}\right)\alpha_2^2 .$$

This implies $\lambda_1 + \lambda_2 + \lambda_3\alpha_1^2 + \lambda_3\alpha_2^2 \ge 0$. Since both trace and determinant of the matrix B_L is non-negative, we have B_L is non-negative definite matrix. Hence, $\text{BT}\big|_{x=L} \ge 0$. We conclude that BT is negative if both conditions are fulfilled.

B Proof of Theorem 6

We use the energy method. Recall that we have $\mathbf{q} = W^{-1}\mathbf{p}$. Multiply (14) by $\mathbf{q}^\top(W^{-1} \otimes P)$ from the left, and adding the transpose we have

$$\begin{aligned}&\frac{d}{dt}\|\mathbf{q}\|_P^2 + \mathbf{q}^\top[\widetilde{M} \otimes (PD + D^\top P)]\mathbf{q} - \mathbf{q}^\top[I \otimes \tfrac{\gamma}{2}P(D_+ - D_-)]\mathbf{q}\\ &= \mathbf{q}^\top(I \otimes P)\text{SAT}.\end{aligned}$$

Note that $\mathbf{q}^\top[I \otimes \frac{\gamma}{2}P(D_+ - D_-)]\mathbf{q} = \langle \mathbf{q}, [I \otimes \frac{\gamma}{2}(D_+ - D_-)]\mathbf{q}\rangle_{W_{\le 0}}$ is negative by choice of D_+ and D_-. Hence, we have

$$\begin{aligned}\mathbf{q}^\top[\widetilde{M} \otimes (PD + D^\top P)]\mathbf{q} &= \mathbf{q}^\top[S\Lambda S^\top \otimes (PD + D^\top P)]\mathbf{q}\\ &= \boldsymbol{w}^\top[\Lambda \otimes (PD + D^\top P)]\boldsymbol{w}\\ &= \boldsymbol{w}^\top(\Lambda \otimes \boldsymbol{e}_N\boldsymbol{e}_N^\top)\boldsymbol{w} - \boldsymbol{w}^\top(\Lambda \otimes \boldsymbol{e}_0\boldsymbol{e}_0^\top)\boldsymbol{w},\end{aligned}$$

where $\boldsymbol{w} = S^\top\tilde{\mathbf{q}}$ and the last equality follows from the SBP property. Hence to have energy non-increasing, we need a negative boundary term:

$$\text{BT}\Big|_{x=L}^{x=0} = \boldsymbol{w}^\top(\Lambda \otimes \boldsymbol{e}_0\boldsymbol{e}_0^\top)\boldsymbol{w} - \boldsymbol{w}^\top(\Lambda \otimes \boldsymbol{e}_N\boldsymbol{e}_N^\top)\boldsymbol{w} + \mathbf{q}^\top(I \otimes P)\text{SAT}. \tag{22}$$

Simplifying further, we have

$$\begin{aligned}\mathrm{BT}\Big|_{x=L}^{x=0} = &\left(\lambda_1 w_1^2 + \lambda_2 w_2^2 + \lambda_3 w_3^2 + \tau_1 w_1(w_1 - \beta_1 w_3) + \tau_2 w_2(w_2 - \beta_2 w_3)\right)\Big|_{x=0} \\ &- \left(\lambda_1 w_1^2 + \lambda_2 w_2^2 + \lambda_3 w_3^2 + \tau_3 w_3(w_3 - \alpha_1 w_1 - \alpha_2 w_2)\right)\Big|_{x=L}.\end{aligned}$$

At $x = 0$, we have

$$\begin{aligned}\mathrm{BT}\Big|_{x=0} = &-\frac{1}{2}\begin{bmatrix} w_1 & w_3 \end{bmatrix}\begin{bmatrix} -2\lambda_1 - 2\tau_1 & \tau_1\beta_1 \\ \tau_1\beta_1 & -\lambda_3 \end{bmatrix}\begin{bmatrix} w_1 \\ w_3 \end{bmatrix} \\ &-\frac{1}{2}\begin{bmatrix} w_2 & w_3 \end{bmatrix}\begin{bmatrix} -2\lambda_2 - 2\tau_2 & \tau_2\beta_2 \\ \tau_2\beta_2 & -\lambda_3 \end{bmatrix}\begin{bmatrix} w_2 \\ w_3 \end{bmatrix}.\end{aligned}$$

The conditions given for τ_1 (18a) and τ_2 (18b) ensure that both of the matrices,

$$\begin{bmatrix} -2\lambda_1 - 2\tau_1 & \tau_1\beta_1 \\ \tau_1\beta_1 & -\lambda_3 \end{bmatrix} \quad \text{and} \quad \begin{bmatrix} -\lambda_3 & \tau_2\beta_2 \\ \tau_2\beta_2 & -2\lambda_2 - 2\tau_2 \end{bmatrix},$$

each have positive trace and determinant, hence both are positive definite.

At $x = L$, we have

$$\mathrm{BT}\Big|_{x=L} = \frac{1}{2}\begin{bmatrix} w_1 & w_2 & w_3 \end{bmatrix}\begin{bmatrix} 2\lambda_1 & 0 & -\tau_3\alpha_1 \\ 0 & 2\lambda_2 & -\tau_3\alpha_2 \\ -\tau_3\alpha_1 & -\tau_3\alpha_2 & 2\lambda_3 + 2\tau_3 \end{bmatrix}\begin{bmatrix} w_1 \\ w_2 \\ w_3 \end{bmatrix}.$$

The condition given for τ_3 (18c) ensures that the determinant of the matrix,

$$\begin{bmatrix} 2\lambda_1 & 0 & -\tau_3\alpha_1 \\ 0 & 2\lambda_2 & -\tau_3\alpha_2 \\ -\tau_3\alpha_1 & -\tau_3\alpha_2 & 2\lambda_3 + 2\tau_3 \end{bmatrix},$$

is positive. Since λ_1 and λ_2 are positive, all leading principal minors of the matrix are positive, hence the matrix is positive definite. We conclude that $\mathrm{BT}\Big|_{x=L}^{x=0}$ is negative, and hence the energy is non-increasing.

Author addresses

1. **Rudi Prihandoko**, Mathematical Science Insitute, The Autralian National University, Australian Capital Teritory 2600, Australia.
mailto:rudi.prihandoko@anu.edu.au
orcid:0000-0001-6376-7952

2. **Stephen Roberts**, Mathematical Science Insitute, The Autralian National University, Australian Capital Teritory 2600, Australia.
mailto:stephen.roberts@anu.edu.au
orcid:0000-0002-6730-3108

3. **Kenneth Duru**, Mathematical Sciences, The University of Texas at El Paso, Texas, USA.
mailto:kduru@utep.edu
orcid:0000-0002-5260-7942

4. **Christopher Zoppou**, Mathematical Science Insitute, The Autralian National University, Australian Capital Teritory 2600, Australia.
mailto:christopher.zoppou@anu.edu.au
orcid:0000-0002-1443-2897

5. **Kenny Wiratama**, Department of Mathematical Sciences, Ulsan National Institute of Science and Technology, Ulsan, South Korea.
mailto:kenny.wiratama@unist.ac.kr
orcid:0000-0003-0475-9180